

## LASER SCANNER SIMULATOR FOR SYSTEM ANALYSIS AND ALGORITHM DEVELOPMENT: A CASE WITH FOREST MEASUREMENTS

Antero Kukko\*, Juha Hyypä

Finnish Geodetic Institute, Department of Remote Sensing and Photogrammetry, P.O. Box 15, 02431 Masala, Finland –  
Antero.Kukko@fgi.fi, Juha.Hyypa@fgi.fi

Commission VI WG VI/4

**KEY WORDS:** Airborne, Terrestrial, Laser scanning, LIDAR, Simulation, Waveform, Quality

### ABSTRACT:

LIDAR systems have come to be extensively used in photogrammetry and mapping sciences. The accuracy of 3D information is mainly affected by navigational and system-dependent uncertainties, but also by the laser beam properties and the nature of the light interaction on the object surface. At the moment, the system-dependent sources of error are much better known than those arising from laser light interaction. In this paper, a simulation approach for scanning LIDAR systems is presented and discussed. Simulating light interaction on an object surface provides an opportunity to measure well-defined objects under controlled conditions. The simulated object remains unchanged over time, and when various sensor and system parameters are applied, it is possible to compare the 3D point clouds created. Furthermore, well-established simulation software makes it possible to study and verify future LIDAR systems and concepts.

### 1. INTRODUCTION

Airborne LIDAR systems have been extensively adopted for mapping purposes in recent years. Uses of laser scanning include digital elevation model (DEM) production (e.g. Kraus and Pfeifer, 1998; Pereira and Janssen, 1999; Axelsson, 2000; Reutebuch et al., 2003), building extraction (e.g. Brenner, 2005; Haala et al. 1998; Hofmann et al. 2002; Hofmann, 2004; Hofton et al., 2000; Maas, 2001; Rottensteiner, 2003; Rottensteiner and Jansa, 2002; Rottensteiner et al. 2005; Vosselman, 2002; Vosselman and Süveg, 2001), and forest management (e.g. Naesset, 2002; Hyypä et al. 2001; Persson et al. 2002; Yu et al. 2004; Matikainen et al., 2003). In these applications the algorithm development is usually based on data retrieved using commercial LIDARs. Consequently, mapping algorithms are often adapted to the laser data used.

Earlier attempts at three-dimensional simulation modeling include modeling of the scanning angle effect in the measurement of tree height and canopy closure in boreal forest with an airborne laser scanner (Holmgren et al. 2003) and the establishment of optimal LIDAR acquisition parameters for forest height retrieval (Lovell et al. 2005). In these cases two assumptions are made: the simulated laser pulse is assumed to be a single ray without any divergence and the coarse objects simulated are assumed to be solid. In general, such simulation methods were useful, but the implementation was relatively simple. Thus, in Holmgren et al. (2003), the simulation method systematically overestimated the laser height percentiles by 2.25 m since beam interaction, waveform, and threshold detection were not simulated.

There are possible applications in which simulation together with good models for the sensors, target and beam interaction would provide further insights. Simulation may also supply answers to some questions, which are not properly understood. Optimization of the laser acquisition parameters is one feasible application area. Opportunities for the use of waveform data has been long delayed due to the lack of experimental data.

However, waveform data can be simulated with some accuracy (Filin & Csathó, 2000; Thiel & Wehr, 2004; Jutzi et al. 2005). Also, the capabilities of future laser instruments can be estimated using simulation and appropriate models.

The quality of products derived from laser scanning is influenced by a number of factors, which can be grouped as follows: errors caused by the laser system (the laser instrument, GPS and INS) and data characteristics (e.g. first/last pulse, point density, flight height, scan angle, beam divergence), errors created during processing of the data (interpolation errors, filtering errors, errors caused by improper break-line detection, segmentation and smoothing of the data), and errors due to characteristics of the target (type and flatness of the terrain, density of the canopy above). By adding simulations to single data experiments, the effect of most of these errors can be estimated in a more reliable way than it is when an experimental approach is adopted.

This article presents ideas and development of a simulation method for existing LIDAR systems, but also general user defined sensors are supported. The purpose of this work is to provide a tool for analyzing systematic properties of scanning LIDAR systems, and factors affecting the quality of the LIDAR end products. Utilization of the simulation method developed also aims at intensifying the algorithm development for specific mapping applications and waveform processing. A case with forest measurements is depicted in more detail.

### 2. LASER SCANNING PRINCIPLE

A laser scanner transmits a short laser pulse, typically 3-10 ns. This laser pulse, or beam, is transmitted in a certain direction to reach the object surface. The beam diverges from its nominal direction and creates a narrow conic shape, and thus the transmitted energy spreads over a larger footprint area. The reflections of the pulse also come from this footprint area and their intensity decreases towards the edges of the beam.

---

\* Corresponding author.

The illuminated footprint area may consist of a variable amount of surface materials at variable ranges and orientations. This affects the power and shape of the backscattered echo, or waveform, of the received signal. This situation is illustrated in Figure 1, which schematically depicts one laser beam and its reflection from a building. The different orientations and locations of the building surfaces cause sequential reflections from the building and ground. The amount of beam divergence from the nominal beam direction causes the decrease in accuracy in both the planar and height directions, since all echoes are considered to be reflected from the axis of the nominal beam direction. A good overview on the basic relations for the laser scanning can be found in (Baltasvias 1999).

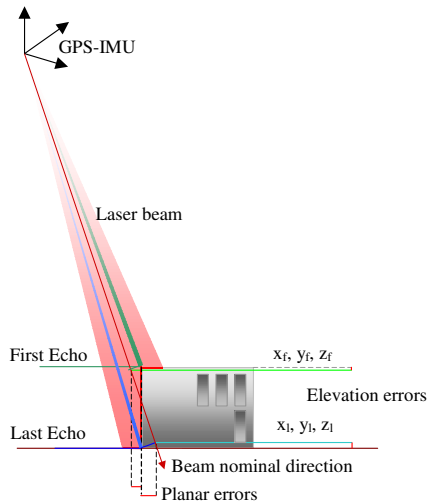


Figure 1. Principle of a LIDAR observation. Beam divergence causes the spread of a beam over the footprint area from which multiple echoes are collected. The nominal beam direction determines the final 3D position.

Three basic scanning geometries are engineered for commercial airborne scanning LIDARs. These operate mainly in line, oscillating (sinusoidal or z-shaped lines) and elliptical geometries, all of which form a different point pattern on the ground. These general patterns are illustrated in Figure 2. The point density on the ground surface is determined by the field of view, pulse repetition rate and scanning frequency as the sensor overflies the area with a known velocity and direction and at a specified altitude.

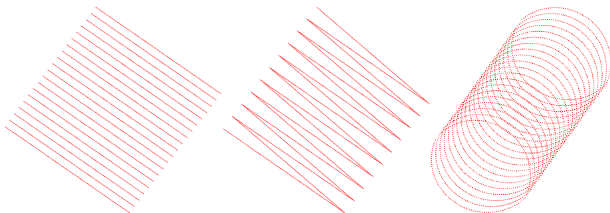


Figure 2. Scanning patterns for three basic measuring principles: A: Line, B: Oscillating, and C: Conic.

Table 1 sums up some principal parameters of commercial airborne laser scanning systems, which are adopted in the simulation software. The main operational differences are in the pulse and scanning frequency, the scanning angle, the beam divergence and the pulse length. It is also expected that the shape of the pulse is different for each of the sensors. The

parameter variability increases if the terrestrial scanners are taken into account, but here they are excluded.

### 3. SIMULATION METHODS

This section describes the basic implementations in the simulation software. The methodology includes emulation of the geometric properties of the scanner system, laser radiation and scattering on the target surface, as well as the signal waveform processing.

A complete LIDAR simulator deals with platform and beam orientation, pulse transmission, beam interaction with the target surface, computation of waveform prototype, and eventually digitization of the waveform:

- Platform and beam orientation – Controls platform movements and scanner operation according to the system and flight parameters.
- Pulse transmission – Deals with the laser beam properties according to the beam angular divergence and the spatial distribution of the transmitted energy.
- Beam interaction – Laser beam division into sub-beams and their interaction with the target surface are computed. Elevation, surface orientation, reflectivity, and distance from the beam center are considered.
- Waveform – The echo waveform prototype is created by summing up the energy returned from different parts of the laser beam according to their range and surface orientation dependent reflectivity. Returned energy is collected by a telescope aperture.
- Threshold detection and waveform digitizing – in this phase the echoes exceeding a given power threshold are detected. Recorded output echo waveform is created in digitization of the simulated echo prototype using system-dependent sampling interval and detection parameters.

#### 3.1 Scanning geometries

Airborne LIDARs typically have three basic scanning geometries, as shown in Figure 2. These are implemented into the simulation software. The other relevant system-specific parameters affecting the achieved scanning pattern, and thus the data coverage on the ground surface, are pulse frequency, scanning rate, scanning angle, and the along track velocity of the platform.

One swath of a scanner consists of a certain amount of beams, defined by the ratio of pulse frequency and scanning rate, and is produced by rotation geometry around the origin of the laser scanner. The field of view of the scanner was divided according to the pre-set parameters to achieve the correct orientation for each beam in the ground coordinate system. Each single laser beam shot was modeled using multiple rays with uniform angular distribution around the center line of sight. The angular separation between adjacent rays, sub-beams, was chosen according to the flight altitude and surface model grid spacing in use.

#### 3.2 Pulse transmission

The power distribution of the transmitted pulse can be approximated by a Gaussian as a function of time. The second element in the transmission sub-system controls the laser beam divergence, in other words, the laser footprint size at ground

Table 1. Characteristics of some commercial airborne laser scanning systems.

Sensor	Mode	Scan Freq.	Pulse Freq.	Scanning Angle	Beam Div. $1/e^2$	Pulse Energy	Range Resolution	Pulse Length	Digitizer
Optech 2033	Oscillating	0-70 Hz	33 kHz	$\pm 20^\circ$	0.2/1.0 mrad	N/A	1.0 cm	8,0 ns	N/A
Optech 3100	Oscillating	0-70 Hz	33-100 kHz	$\pm 25^\circ$	0.3/0.8 mrad	<200 $\mu$ J	1.0 cm	8,0 ns	1 ns
TopEye MkII	Conic	35 Hz	5-50 kHz	14°, 20°	1.0 mrad	N/A	<1.0 cm	4,0 ns	0.5 ns
TopoSys I	Line	653 Hz	83 kHz	$\pm 7.15^\circ$	1.0 mrad	N/A	6.0 cm	5,0 ns	N/A
TopoSys II Falcon	Line	630 Hz	83 kHz	$\pm 7.15^\circ$	1.0 mrad	N/A	2.0 cm	5,0 ns	1 ns
Leica ALS50	Oscillating	25-70 Hz	83 kHz	$\pm 37.5^\circ$	0.33 mrad	N/A	N/A	10 ns	N/A
Leica ALS50-II	Oscillating	35-90 Hz	150 kHz	$\pm 37.5^\circ$	0.22 mrad	N/A	N/A	10 ns	1 ns
LMS-Q560	Line	160 Hz	<100 kHz	$\pm 22.5^\circ$	0.5 mrad	8 $\mu$ J	2.0 cm	4,0 ns	1 ns

level. The size of the footprint on the ground is a simple function of the divergence angle and the flight altitude, or more precisely the range:

$$D = 2z \tan \Delta\theta/2, \quad (1)$$

where  $D$  is the beam footprint diameter,  $\Delta\theta$  is the beam divergence angle and  $z$  the distance to the ground surface.

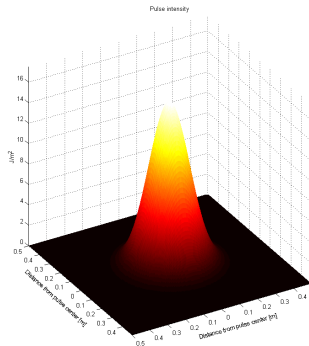


Figure 3. Intensity pattern of a 8  $\mu$ J Gaussian TEM<sub>00</sub> pulse with a beam divergence angle of 1.0 mrad ( $1/e^2$ ) at range of 400 m. The resulting footprint diameter is approximately 40 cm.

The intensity of a laser pulse is modeled using transverse mode TEM<sub>00</sub>, which gives one centralized Gaussian spot on the target surface. As it travels in the air, the laser-beam wavefront acquires curvature and begins to spread as follows:

$$w(z) = w_0 \left[ 1 + \left( \frac{\lambda z}{\pi w_0^2} \right)^2 \right]^{1/2}, \quad (2)$$

where  $z$  is the distance propagated from the plane where the wavefront was flat,  $\lambda$  is the wavelength of light,  $w_0$  is the radius of the  $1/e^2$  irradiance contour at the plane where the wavefront is flat,  $w(z)$  is the radius of the  $1/e^2$  contour after the wave has

propagated a distance  $z$ . Eventually attained energy per unit area is:

$$I(r) = \frac{2P}{\pi w^2} \exp\left(\frac{-2r^2}{w^2}\right), \quad (3)$$

where  $I(r)$  is the intensity function,  $P$  the total energy,  $w$  the laser footprint radius measured between  $\pm 2\sigma$  points, and  $r$  the distance from the centre of the laser beam. Thus, the energy decreases as a function of the distance from the beam centre leading to less energy returning from the outer parts of the beam than from the centre. Intensity pattern of a typical airborne laser scanner pulse is illustrated in Figure 3.

The transmitted laser pulse is modeled by a predefined number of discrete rays. The returned energy is calculated using the intensity of the transmitted pulse at the range in question, the surface reflectivity and the area of interaction, which here depends on the beam sub-division parameters:

$$E_{ret}(r) = \tau R(\theta) I_0(r) A, \quad (4)$$

where  $E_{ret}$  is the returned energy,  $\tau$  is atmospheric transmission,  $R$  anisotropic surface reflectance at given angle of incidence  $\theta$ ,  $I_0$  pulse intensity at range  $r$  from the scanner, and  $A$  the receiving area of the scatterer. Surface reflectance  $R$  depends on the angle of incidence  $\theta$ , and the type of the surface. Scatterer cross section area  $A$  was calculated using angular distribution of sub-beam rays. Each scatterer (ray intersection) is then summed to an echo waveform prototype. Finally, the recorded intensity is affected by the aperture of the receiver telescope.

### 3.3 Scattering and attenuation

The wavelength of the laser used affects the scattering from the object surface. This scattering can be assumed to be isotropic, but the anisotropy should be taken into account for better precision. Scattering anisotropy depends greatly on the surface orientation relative to the light source, and on the surface

properties (Nicodemus et al., 1977; Hapke et al., 1996; Sandmeier and Itten, 1999).

Variation in the light scattering from different surfaces can be carried out by introducing different object types and incidence angle dependent scattering functions. Models introducing multiple scattering could also be considered. In this paper, the scattering was assumed to conform to the cosine of the angle of incidence. Laboratory measurements of backscattered intensity as a function of the angle of incidence using 1064 nm laser light have been performed for a set of natural and artificial surface types, and the data are being processed for description and use in a future paper. It is an interesting question, how much this kind of behaviour affects the accuracy of LIDAR range measurement.

Atmospheric transmission is of little interest within this context, since it can simply be considered constant, and thus only adds a scale term to the simulated energy, not altering the shape of the recorded waveform. This should be taken into account when data acquired using different flight altitudes and possible wavelengths are compared.

### 3.4 Waveform sampling

The transmitted pulse was modeled as energy vs. time function, with known time interval sampling. For simulation purposes 100 ps sampling was chosen to obtain the prototype echo waveform. This provides time sampling that is 5-10 times better than that provided by widely available scanners.

Every sub-beam of a modeled laser beam results in a distance, or range, from scanner to target surface. Thus one beam results in a number of distance measurements. Ranges are converted into time units and sub-echoes are summed into a sum echo as a function of time according to their scattering angle dependent reflectance. By summing up all the sub-echoes we obtain a sum waveform, including approximated noise, at a given 100 ps sampling interval. This provides a high-resolution view of the target, which could be regarded as an approximation of its physical properties.

The output echo waveform is then digitized from the higher resolution prototype waveform with a given system dependent sampling. By using the detector threshold, the information exceeding the selected noise level is found and digitized. This gives the first approximation for the point location, but more importantly captures the meaningful signal from the time slot. The recorded waveform is though more often analyzed in post processing, and could be used for more exact point extraction and range detection algorithm development.

One of the most crucial factors for exact range determination is the echo detection algorithm applied (Wagner et al., 2004, Wagner, 2005). Since the length of the laser pulse is longer than the accuracy needed (a few meters versus a few centimeters), a specific timing of the return pulse needs to be defined.

In a non-waveform ranging system, analogue detectors are used to derive discrete, time-stamped trigger pulses from the received signal in real time during the acquisition process (Wagner, 2005). The timing event should not change when the level of signal varies, which is an important requirement in the design of analog detections as discussed by (Palojärvi, 2003). For full-waveform digitizing ALS systems several algorithms can be used at the post-processing stage (e.g. leading edge

discriminator/threshold, center of gravity, maximum, zero crossing of the second derivative, and constant fraction) (Wagner, 2005).

The most basic technique for pulse detection is to trigger a pulse whenever the rising edge of the signal exceeds a given threshold (leading edge discriminator), which was also implemented in this first version of the simulation system. Although it is conceptually simple and easy to implement, this approach suffers from a serious drawback: the timing of the triggered pulse (and thus the distance measurement) is rather sensitive to the amplitude and width of the signal. If the amplitude of the pulse changes then the timing point also changes. The same applies for the center of gravity when computed over all points above a fixed threshold.

More sophisticated schemes are based on finite differences of numerical derivatives (e.g. the detection of local maxima or the zero crossings of the second derivative) or, more generally, the zero-crossings of a linear combination of time-shifted versions of the signal. An example of the latter approach is the constant fraction discriminator, which determines the zero crossings of the difference between an attenuated and a time-delayed version of the signal (Gedcke and McDonald, 1968). Maximum, zero crossing, and constant fraction are invariant with respect to amplitude variations and therefore also, to some degree, changes in pulse width (Wagner, 2005).

### 3.5 Surface and object models

In this paper, the surfaces used for simulation were modeled as high-resolution rasters. A grid spacing of a few centimeters was used. The height resolution of the models was 1.0 cm. Artificial building and forest models, and those based on multiple overlapping laser scanning strips, were used. Artificial models consist of areas much smaller than those in natural test areas, for example single buildings or a randomly generated forest stand as seen in Figure 4, which presents a forest canopy model expressing deciduous forest, 150x150 m<sup>2</sup> in area.

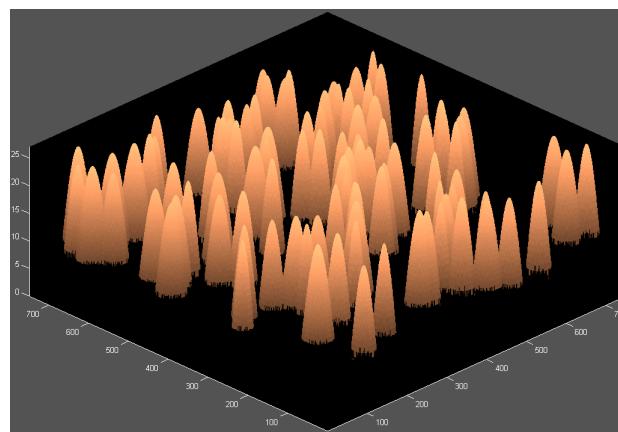


Figure 4. Randomly generated forest canopy model.

## 4. TESTS AND RESULTS

In this section we present one case, which demonstrate the versatility of the developed simulator in an airborne forest mapping, as the forest parameter extraction using LIDAR techniques is common practice nowadays. Here we present some preliminary results achieved by simulating TopEye MK-II laser scanner over a model forest 150x150 m<sup>2</sup> in size. The

total number of trees was 100, with a mean height of 25.97 m and a standard deviation of 0.58 m. The tree crowns were characterized by a 10.31 m mean crown diameter with 1.40 m deviation, and modeled by means of a sinusoidal surface with 5.0 cm grid spacing,

The simulated data presented in Figure 5 was acquired at an altitude of 200 m, and a flight speed of 25 m/s. The pulse repetition frequency was set at 30kHz, and the scanning angle at 20 degrees. The sub-sampling of the 1.0 mrad laser beam was set according to the model grid spacing and the flight altitude used, thus giving 53 sub-beams within the foot print area of 20 cm in diameter at ground level. Furthermore, a constant detector energy threshold was used to extract the first echo 3D-points from the 1.0 GHz sampled waveform data produced by the simulator.

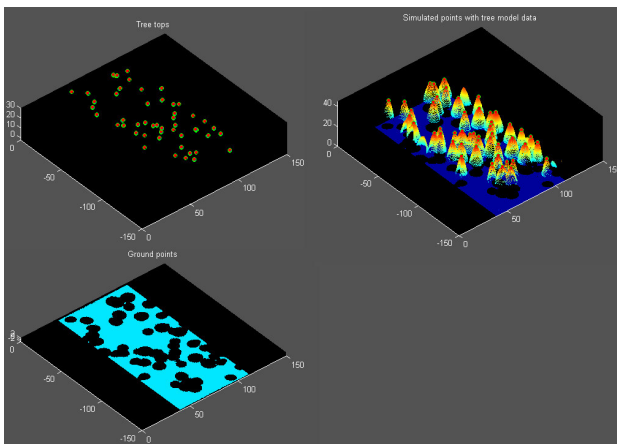


Figure 5. Composite presentation of the simulated measurements for a forest model. The tree tops of the forest model (top left), the tree tops expressed on top of the simulated points (top right), and ground points extracted from the simulated data (bottom left).

The tree tops were extracted from the simulated data using a priori model information on the tree locations. The maximum height point within a 0.5 m radius of the model tree top was chosen. On average this tree top estimator indicates a 0.33 m underestimation of the tree heights compared with the known ground level in the model. When simulated ground points within a one-meter wide circular belt around the tree canopy were considered, the tree height underestimation decreased to 0.02 m. This could be explained by the fact that the model trees had relatively flat tops with approximately the same surface orientation as the ground surface around the trees. Also, no distinction was made between the tree canopy and the ground reflectivities.

Tree location was extracted to 0.15 m accuracy by considering the selected maximum height point as a good representative. This was a rather good estimation thanks to the relatively dense point spacing and smooth shape of the tree canopy model. According to the international Tree Extraction comparison (Hyyppä and Kaartinen, 2007), the best models using a point density of 2-8 pt/m<sup>2</sup> resulted in a median error of 0.5 m in location. However, in this study the segmentation errors of individual trees were the main source of errors. Also, the tree trunks were not always vertical.

Based on this test case it is clear that this novel simulation method provides reasonable and accurate results for forest parameter extraction, compared with those presented by Holmgren et al. (2003) and Lovell et al. (2005). The advantages lie in the modeled beam divergence, and in the consideration of the incidence angle effect and waveform detection.

The full capability of the simulation system is expressed by a simulation over a ground model based on multi-strip point data acquired with TopoSys Falcon in August 2006. The simulated data were acquired using system characteristic parameter values for the Optech ALTM 3100 and TopoSys Falcon determining the spatial distribution of the laser beams, pulse transmission and waveform detection. The resulting simulated point cloud data and detailed profile for data comparison are presented in Figure 6, along with the original point data, in which the point colors are coded by elevation.

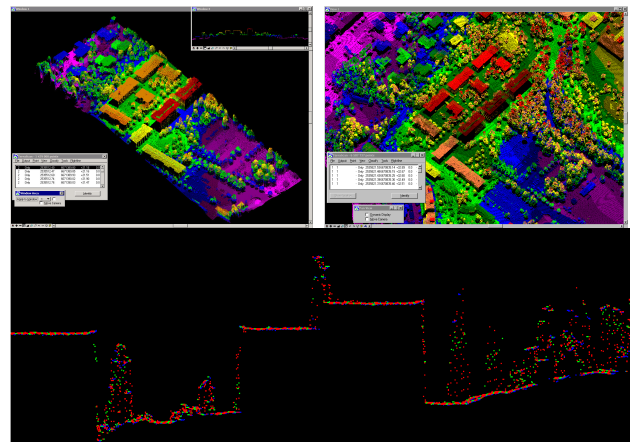


Figure 6. Point cloud presentation of the simulated data (top left) and the original laser scanning data (top right). Comparison of the original data (blue) with the simulated TopoSys Falcon (green) and Optech ALTM 3100 (red).

The level of details in the original first pulse data is reproduced by the simulation. The point spacing and elevation information are comparable to the original. The differences in the color mapping in Figure 6 are due to the larger elevation range of the original data as the data area is larger. More comparative statistical data analysis is beyond the scope of this issue.

The simulation method developed was intended to be a universal tool for studies on multiple parameters affecting the laser scanning accuracy and end products. This kind of approach is suggested for use in finding relevant system dependent differences affecting the data quality and suitability for desired mapping tasks. Simulation also makes it possible to better understand the particular measurement technique and its properties.

## 5. CONCLUSIONS

In this paper the simulation approach to laser scanning data is introduced and discussed. The simulation method implemented is the first to combine both spatial and radiometric components to produce realistic point cloud and waveform data for system analysis and algorithm development. Simulation provides a tool for demonstrating the effect of different factors on a LIDAR measurement. When integrated into an implementation of

sensor and platform geometry, simulation is a powerful tool for verification and comparison of different laser scanning systems, and analysis of the technique itself. Furthermore, simulator provides artificial data on known targets for algorithm development purposes in many fields of application. It is also clear that simulation of this kind is an important adjunct to the analytical error modeling and estimation performed creditably in recent years (Balsavias, 1999; Schenk, 2001; Wagner et al., 2006).

Preliminary results show that different system-dependent factors affecting the quality of LIDAR-based end products can be studied by simulation. It is also expected that the applicability of the simulation in this kind of research will be very varied. Since simulation makes it possible to acquire data from an unchanged object with different scanning geometries, it is possible to perform thorough analysis of the effect of scanning geometry on the quality of laser products. This is not usually possible with the real data.

Simulation provides a promising and efficient method for studying application-dependent parameters to optimally fulfill the demands of different LIDAR mapping tasks. Greater understanding of the particular measurement technique and its properties is possible. This kind of approach could be used to find relevant system-dependent differences affecting data quality and suitability for desired mapping tasks. Furthermore, the effects of positioning and scanner inaccuracies can be studied by varying the magnitude of these errors, or alternatively they can be completely omitted and attention given only to instrument-dependent sources of uncertainty in the data.

Further development of the LIDAR simulation method will deal with more precise scattering models as the results of the laboratory measurements become available.

#### ACKNOWLEDGEMENTS

Academy of Finland, Jenny and Antti Wihuri Foundation and Finnish Foundation of Technology are gratefully acknowledged for their financial support. Dr. Sanna Kaasalainen is acknowledged for her valuable comments.

#### REFERENCES

- Axelsson, P., 2000. DEM generation from laser scanner data using adaptive TIN models. *International Archives of Photogrammetry and Remote Sensing*, XXXIII, Part B4, Amsterdam, Netherlands.
- Balsavias, E.P., 1999. Airborne Laser scanning: basic relations and formulas. *ISPRS Journal of Photogrammetry and Remote Sensing*, 54 (2/3), 199-214.
- Brenner, C., 2005. Building reconstruction from images and laser scanning. *International Journal of Applied Earth Observation and Geoinformation* 6(3-4), 187-198.
- Filin, S. & B. Csathó, 2000. An efficient algorithm for the synthesis of laser altimetry waveforms. Byrd Polar Research Center, Technical Report 2000-2.
- Gomes-Pereira, L. & L. Janssen, 1999. Suitability of laser data for dtm generation: A case study in the context of road planning and design. *ISPRS Journal of Photogrammetry and Remote Sensing*, 54, 244-253.
- Haala, N., Brenner, C. & K.-H. Anders, 1998. 3D urban GIS from laser altimeter and 2D map data. In: *International Archives for Photogrammetry and Remote Sensing (IAPRS)*, Columbus, Ohio, XXXII, Part 3/1, 339-346.
- Hapke, B., DiMucci, D., Nelson, R., Smythe, W., 1996. The cause of the hot spot in vegetation canopies and soils; shadow-hiding versus coherent backscatter. *Remote Sensing of Environment*, 58, pp. 63-68.
- Hofmann, A. D., Maas, H.-G. & A. Streilein, 2002. Knowledge-Based Building Detection Based On Laser Scanner Data And Topographic Map Information, *Symposium on Photogrammetric Computer Vision, ISPRS Commission III*, September 9 - 13, 2002, Graz, Austria.
- Hofmann, A.D. 2004. Analysis of TIN-structure parameter spaces in airborne laser scanner data for 3-D building model generation, *International Archives of Photogrammetry and Remote Sensing*, 35, B3 III, 302-307.
- Hofton, M. A., Blair, J. B., Minster, J.-B., Ridgway, J. R., Williams, N. P., Bufton, J. L. & D. L. Rabine, 2000. An Airborne Scanning Laser Altimetry Survey Of Long Valley, California. *International Journal of Remote Sensing*, 21(12), 2413-2437.
- Holmgren, J., Nilsson, M. & H. Olsson, 2003. Simulating the effects of lidar scanning angle for estimation of mean tree height and canopy closure. *Canadian Journal of Remote Sensing*, 29 (5), 623-632.
- Hyypä, J. & H. Kaartinen, 2007. Tree extraction comparison, To be published in EuroSDR report series, manuscript in preparation.
- Hyypä, J., Kelle, O., Lehtikoinen, M., & M. Inkinen, 2001. A segmentation-based method to retrieve stem volume estimates from 3-D tree height models produced by laser scanners. *IEEE Transactions on Geoscience and Remote Sensing*, 39(5), 969-975.
- Jutzi, B., Neulist, J., & U. Stilla, 2005. High-resolution waveform acquisition and analysis of laser pulses. *ISPRS Hannover Workshop 2005 'High-Resolution Earth Imaging for Geospatial Information'*, Hannover, Germany, 17-20 May 2005.
- Kraus, K., & N. Pfeifer, 1998. Determination Of Terrain Models In Wooded Areas With Airborne Laser Scanning Data. *ISPRS Journal of Photogrammetry and Remote Sensing*, 53 (4), 193-203.
- Lovell, J.L., Jupp, D.L.B., Newnham, G.J., Coops, N.C. & D.S. Culvenor, 2005. Simulation study for finding optimal lidar acquisition parameters for forest height retrieval. *Forest Ecology and Management*, 214, 398-412.
- Maas, H. G., 2001. The suitability of airborne laser scanner data for automatic 3D object reconstruction. In: Balsavias, E. P., Gruen, A., Van Gool, L. (eds): *Automatic Extraction of Man-made Objects From Aerial and Space Images (III)*, Lisse, Balkema.
- Matikainen, L., Hyypä, J., & H., Hyypä, 2003. Automatic detection of buildings from laser scanner data for map updating. In: *International Archives of Photogrammetry, Remote Sensing and Spatial Information Sciences, Dresden, Germany, Vol. XXXIV, Part 3/W13*, 218-224.

- Montemerlo, M., Thrun, S., Dahlkamp, H., Stavens, D. & S. Strohband, 2006. Winning the DARPA Grand Challenge with an AI Robot. Proceedings of the 21st National Conference on Artificial Intelligence AAAI-06, July 16–20, Boston, Massachusetts.
- Nelson, R., 1997. Modeling forest canopy heights: The effects of canopy shape. *Remote Sensing of Environment*, 60, 237-334.
- Naesset, E., 2002. Predicting forest stand characteristics with airborne scanning laser using a practical two-stage procedure and field data. *Remote Sensing Environment*, 80, 88–99.
- Nicodemus, F. E., Richmond, J. C., Hsia, J. J., 1977. Geometrical considerations and nomenclature for reflectance. U.S. National Bureau of Standards Monograph 160.
- Persson, Å., Holmgren, J. & U. Söderman, 2002. Detecting and measuring individual trees using an airborne laser scanner. *Photogrammetric Engineering and Remote Sensing*, 68, 925-932.
- Reutebuch, S., R. McGaughey, H-E Andersen, and W. Carson, 2003. Accuracy of a high resolution LIDAR-based terrain model under a conifer forest canopy. *Canadian Journal of Remote Sensing*, 29, 527-535.
- Rottensteiner, F., 2003. Automatic Generation of High-Quality Building Models from Lidar Data. *IEEE Computer Graphics and Applications*, 23(6), 42 – 50.
- Rottensteiner, F. & J. Jansa, 2002. Automatic Extraction of Buildings from Lidar Data and Aerial Images. Commission IV Symposium "Geospatial Theory, Processing and Applications" - WG3, Ottawa, Canada, 34(3).
- Rottensteiner, F., Trinder, J. & S. Clode, 2005. Data Acquisition for 3D City Models from LIDAR - Extracting Buildings and Roads. Proceedings of the 25th IEEE International Geoscience And Remote Sensing Symposium (IGARSS), July 25-29, Seoul, South Korea, 521-524.
- Rönnholm, P., Hyypä, J., Hyypä, H., Haggrén, H., Yu, X. & H. Kaartinen, 2004. Calibration of laser-derived tree height estimates by means of photogrammetric techniques. *Scandinavian Journal of Forest Research* 19(6), 524-528.
- Sandmeier, S., Itten, K., 1999. A field goniometer system (FIGOS) for acquisition of hyperspectral BRDF data. *IEEE Transactions on Geosciences and Remote Sensing*, 37 (2), pp. 978-986.
- Schenk, T., 2001. Modeling and analyzing systematic errors in airborne laser scanners. Technical notes in photogrammetry No. 19, Department of Civil and Environmental Engineering and Geodetic Science, The Ohio State University, Columbus, OH.
- Talaya, J., Bosch, E., Alamús, R., Bosch, E., Serra, A. & A. Baron, 2004. GEOMOBIL: the Mobile Mapping System from the ICC. In: Proceedings of 4th International Symposium on Mobile Mapping Technology (MMT'2004). Kinming, China.
- Thiel, K.-H. & A. Wehr, 2004. Performance capabilities of laser scanners – an overview and measurement principle analysis. *International Archives of Photogrammetry Remote Sensing and Spatial Information Sciences*, XXXVI-8/W2, 14-18.
- Vosselman, G., 2002. Fusion of Laser Scanning Data, Maps and Aerial Photographs for Building Reconstruction. *IEEE International Geoscience and Remote Sensing Symposium and the 24th Canadian Symposium on Remote Sensing, IGARSS'02*, Toronto, Canada, June 24-28.
- Vosselman, G. & I. Suveg, 2001. Map Based Building Reconstruction from Laser Data and Images. *Automatic Extraction of Man-Made Objects from Aerial and Space Images (III)*, Ascona, Switzerland, June 11-15, Balkema Publishers, 231-239.
- Wagner, W., Ulrich, A., Ducic, V., Melzer, T., & N. Studnicka, 2006. Gaussian Decomposition and Calibration of a Novel Small-Footprint Full-Waveform Digitising Airborne Laser Scanner. *ISPRS Journal of Photogrammetry and Remote Sensing*, 60 (2), 100 - 112.
- Yu, X., Hyypä, J., Kaartinen, H., & M. Maltamo, 2004. Automatic detection of harvested trees and determination of forest growth using airborne laser scanner, *Remote Sensing of Environment*, 90, 451-462.